PERGAMON

Vision Research 41 (2001) 2733–2739

Vision Research

www.elsevier.com/locate/visres

3D after-effects are due to shape and not disparity adaptation

Fulvio Domini [a,*], Wendy Adams [b], Martin S. Banks [c]

[a] *Department of Cognitive and Linguistic Sciences, Brown University, Providence, RI 02912, USA*
[b] *Department of Psychology, University of Glasgow, Glasgow, UK*
[c] *Optometry, Vision Science, and Psychology, University of California, Berkeley, CA, USA*

Received 29 March 2000; received in revised form 2 January 2001

Abstract

There are a variety of stereoscopic after-effects in which exposure to a stimulus with a particular slant or curvature affects the perceived slant or curvature of a subsequently presented stimulus. These after-effects have been explained as a consequence of fatigue (a decrease in responsiveness) among neural mechanisms that are tuned to particular disparities or patterns of disparity. In fact, a given disparity pattern is consistent with numerous slants or curvatures; to determine slant or curvature, the visual system must take the viewing distance into account. We took advantage of this property to examine whether the mechanisms underlying the stereoscopic curvature after-effect are tuned to particular disparity patterns or to some other property such as surface curvature. The results clearly support the second hypothesis. Thus, 3D after-effects appear to be caused by adaptation among mechanisms specifying surface shape rather than among mechanisms signaling the disparity pattern.

Keywords: Vision; Depth; Stereo; After-effect

1. Introduction

Visual after-effects have been very useful in examining the properties of neural mechanisms in the human visual system (McCollough, 1965). These after-effects are generally explained as a by-product of fatigue among neural mechanisms that respond to a particular stimulus dimension. Fig. 1 demonstrates one interesting after-effect. The upper figure is a stereogram that, when fused, looks like a flat surface. The lower figure is another stereogram that looks like a concave surface. Inspect the lower figure for 30 s or so, and then look at the upper figure: it now appears convex. Adaptation to the concave surface causes a change in the perceived curvature of the nominally flat surface.

This and other stereoscopic after-effects have been explained as the consequence of fatigue among neural mechanisms tuned to different patterns of disparity (Koehler & Emery, 1947; Long & Over, 1973; Howard & Rogers, 1995). An example is the study by Long and Over (1973) in which observers adapted to a disparate square. If the adapting square had been in front of the fixation plane (crossed disparity), a subsequently viewed square in the plane of fixation (i.e. zero disparity) was perceived behind the fixation plane. Similarly, if the disparate adapting square had been behind (uncrossed disparity), then the subsequently viewed square appeared to be in front of the fixation plane. Long and Over explained this after-effect with a two-channel mechanism, one with crossed-disparity detectors and the other with uncrossed. Before adaptation, the activities of these two sets of detectors are balanced and, consequently, a zero-disparity stimulus is perceived in the fixation plane. However, when the observer adapts to a square in front of fixation, the crossed-disparity mechanism is fatigued, and its sensitivity is reduced. This creates a temporary imbalance in the two-channel mechanism, and the crossed disparity mechanism responds less than the uncrossed mechanism when presented a zero-disparity square. As a consequence, the zero-disparity square appears behind fixation. Howard and Rogers (1995) and others proposed a similar model based on multiple channels.

* Corresponding author. Tel.: +1-401-863-1356; fax: +1-401-863-2255.
E-mail address: fulvio_domini@brown.edu (F. Domini).

0042-6989/01/$ - see front matter
PII: S0042-6989(01)00161-4

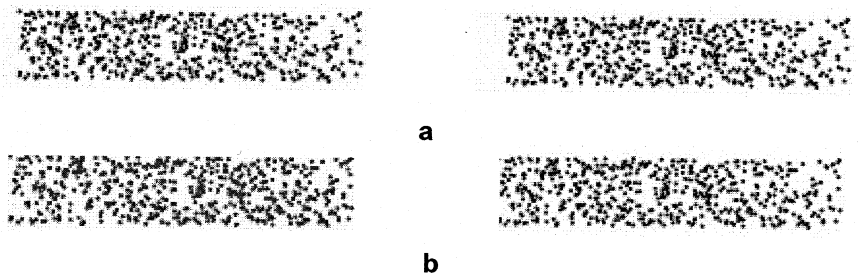

Fig. 1. Curvature after-effect. (a) Random-dot stereogram specifying a flat surface (at the correct viewing distance). (b) Stereogram specifying a concave surface. To fuse the stereograms, the left eye should be directed toward the right half image and vice versa. To experience the curvature after-effect, place a sheet of paper such that it covers the upper stereogram. Fixate the lower stereogram for 30 s (holding fixation near the center of the stimulus), and then look at the upper stereogram; it will appear convex. The change in the apparent curvature of the upper surface is the curvature after-effect.

The two-channel and multi-channel models have been used to explain stereo after-effects in terms of adaptation to absolute disparities. However, there is empirical evidence that the visual system uses relative disparities in recovering surface slant and curvature (reviewed by Howard & Rogers, 1995). For example, Ryan and Gillam (1993) reported a stereoscopic after-effect of adaptation to a disparity gradient (first-order disparity associated with a slanted plane), and te Pas, Rogers, and Ledgeway (1997) reported an after-effect of adaptation to a second-order disparity (associated with curvature).

In summary, empirical results on stereo adaptation have been explained so far by models that postulate the existence of mechanisms coding particular disparities or disparity patterns. In research reported here, we show that curvature after-effects (Fig. 1) cannot be explained solely by adaptation among mechanisms tuned to patterns of retinal disparity. Rather, curvature after-effects seem to be the result of adaptation to mechanisms tuned to surface curvature. To show this, we used a technique that allows one to separate the simulated 3D curvature of a stereo surface from the second-order disparities. In particular, we will show that the same retinal-disparity patterns can have different adaptation effects depending on the perceived curvature produced by the disparity patterns.

1.1. Shape-curvature versus disparity-curvature

To demonstrate how 2nd-order disparity can be differentiated from shape curvature, let us consider a property of curved surfaces described by von Helmholtz (1909) and Ogle (1950). The curved surfaces are conic sections (circles, ellipses, and hyperbolae). They pass through the fixation point and the centers of the two eyes (Fig. 2a). Conic sections create patterns of horizontal disparities that can be characterized by a single value:

$$H = \cot\alpha_R - \cot\alpha_L \quad (1)$$

where α_L and α_R are the horizontal angles subtended at the left and right eyes by the fixation point and any other point on the surface (Fig. 2a). For a given H, the second spatial derivative of disparity (2nd-order disparity) is constant. Fig. 2b shows how the same value of H, and therefore, the same 2nd-order disparity can be

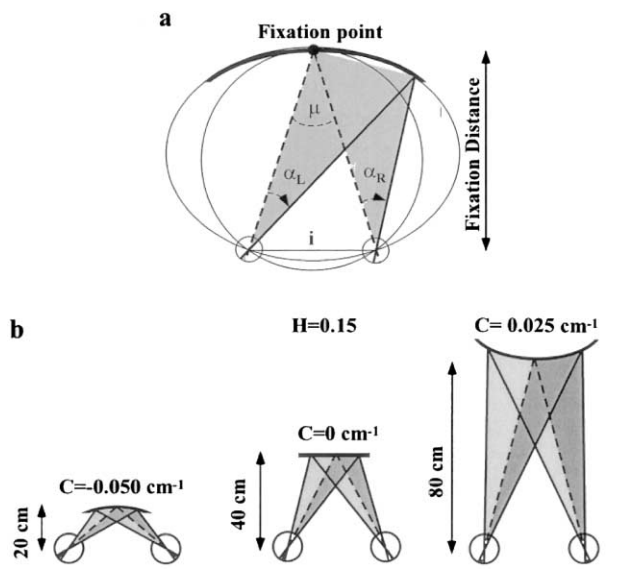

Fig. 2. Binocular viewing geometry for conic sections. (a) Retinal disparity between two points is the difference between the angles subtended by the points at the two eyes. The angles α_L and α_R are subtended at the left and right eyes, respectively. The eyes are directed toward the fixation point, so $\alpha_L - \alpha_R$ is the absolute disparity of the second point. i is the interocular distance, and p is the vergence (the angle between the lines of sight). The circle going through the eyes and fixation point is the Vieth–Muller circle. The ellipse is another conic section encompassing the eyes and fixation point. If the fixation point and other points lie on a conic section (ellipse, circle, plane, hyperbola), the absolute disparities of the points can be specified by one number: $H = \cot\alpha_R - \cot$; in other words, all points on a conic section (such as the thick curve) satisfy that equation. (b) Relationship between H and surface curvature. The left, middle and right panels show the surfaces that yield $H = 0.15$ at 20, 40 and 80 cm, respectively. Notice that their curvatures are very different: the surface creating that pattern of disparities is concave at 20 cm, flat at 40 cm and convex at 80 cm.

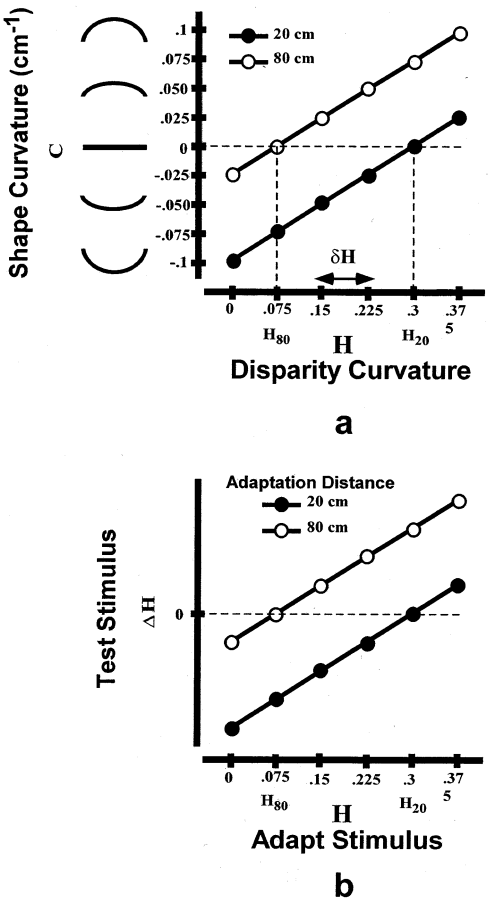

Fig. 3. Disparity vs. curvature and predictions. (a) Local curvature at the fixation point (from Eq. (2)) as a function of H for fixation distances of 20 cm (filled circles) and 80 cm (open circles). (b) Qualitative predictions of the curvature model in terms of the difference in the H value that looked planar before and after adaptation (ΔH) as a function of the adapting H and viewing distance.

produced by the retinal projection of 3D surfaces with different curvatures. The 2nd-order disparity is the same in each case ($H = 0.15$), but the disparity specifies different curvatures at the three distances. When the distance is equal to i/H (where i is interocular distance), the surface is flat (Ogle, 1950). Thus, the pattern of horizontal disparities is insufficient to specity surface shape; the distance must also be measured (Ogle, 1950; Rogers & Bradshaw, 1995).

The relationship between 2nd-order disparity (H) and the local curvature (C) of the surface is given by:

$$C = \frac{1}{i}\frac{4\tan(\mu/2)}{(1+\tan(\mu/2)^2)}\left(\frac{H}{2\tan(\mu/2)} - 1\right) \quad (2)$$

where C is the curvature (reciprocal of radius) at the fixation point (which lies straight ahead in the head's median plane), i is the interocular distance and μ is the angle between the lines of sight (the vergence angle). If the vergence angle is small, $\tan(\mu/2) \approx \mu/2$ and $\tan(\mu/2)^2 \ll 1$, Eq. (2) reduces to:

$$C \approx \frac{2}{i}(H - \mu). \quad (3)$$

Fig. 3A shows the relationship between disparity curvature and shape (Eq. (3)). The upper line represents the relationship for a viewing distance of 20 cm and the lower line for a distance of 80 cm. For a given distance, the relationship between H and the local curvature is nearly linear. Starting with a negative value, increases in H correspond to a changing curvature from convex to flat to concave. More importantly, notice that the H value corresponding to flat differs with viewing distance. From Eq. (3), the value associated with flatness is approximately the vergence angle (μ). If we assume an inter-ocular distance of 6 cm, an H value of 0.075 corresponds to a flat surface at 80 cm, whereas the same value corresponds to a convex surface at 20 cm. Usually observers' percepts will differ from the physically specified shape (because there are other, contradictory cues to distance), so the H value corresponding to a perceived flat surface will not be exactly equal to μ. We will, therefore, refer to the H values that appear planar at vergence distances of 20 and 80 cm as H_{20} and H_{80}. If we indicate these values simply as H_{flat}, Eq. (3) becomes:

$$C \approx \frac{2}{i}(H - H_{\text{flat}}). \quad (4)$$

The function relating H and curvature is nearly linear, so adding an H increment (δH) to the 'flat' value will yield a roughly equivalent change in perceived curvature at all viewing distances. Therefore, $H_{80} + \delta H$ and $H_{20} + \delta H$ will appear to have roughly the same (concave) curvature ($C = 0.025$ cm^{-1}). By using various combinations of H and viewing distance, we can dissociate 2nd-order disparity and perceived curvature.

1.2. Adapation to 3D curvature or retinal disparities?

We ask here whether curvature after-effects are due to adaptation of mechanisms tuned to retinal disparities (or disparity patterns) or higher-level mechanisms tuned to perceived 3D curvature. In the former case, the 2nd-order disparity (H) is the relevant stimulus dimension for predicting the after-effect; in the latter case, the perceived curvature (C) is the relevant dimension. In the experiment reported here, observers adapted to different H values at two viewing distances (the circles on Fig. 3a represent the entire set of adapting stimuli). Following adaptation, they adjusted the H value of a test stimulus until it appeared planar. In half of the trials, the distance to the test stimulus was the same as the distance to the adaptation stimulus, and in the other half, it was different. If adaptation takes place, then the H value corresponding to a perceived 3D planar surface is different from the pre-adaptation H_{flat}. Let us say, for example, that a stimulus that appeared

flat before adaptation appears convex after adaptation. In order to make this stimulus appear flat, the observer must increase the H value to compensate for the apparent convexity. The new H value, therefore, must be larger than H_{flat}. In this case, $\Delta H = H - H_{\text{flat}}$ is positive.

The issue under examination is the stimulus dimension to which the mechanisms underlying 3D shape after-effects respond. Mechanisms that respond differentially to disparity (and disparity gradients) will produce different after-effects than mechanisms that respond differentially to surface curvature. We refer to the former as the *disparity model* and the latter as the *curvature model*. According to the disparity model, the after-effect, measured using the test stimulus, is determined only by the disparity patterns of the adaptation and test stimuli (both quantified by B). For example, it predicts an after-effect of an increase in perceived convexity of the test stimulus when the adaptation stimulus has a negative H value (or some value smaller than the 'null' or 'normalization' value). There should be no effect of distance to the test or adaptation stimulus. According to the curvature model, the perceived shape of the test stimulus after adaptation will be affected by the perceived curvature of the adaptation stimulus (and not by the disparity pattern per se). Thus, the model predicts an after-effect of an increase in perceived convexity when the adaptation stimulus is concave, whether its H value is positive, zero, or negative. Because perceived shape depends on both H and distance, the curvature model predicts that the after-effect will be affected by the vergence distance to the adaptation stimulus. If, for example, the observer adapts to H_{20} viewed at 20 cm, no after-effect should be expected since the adaptation surface is perceived as flat, and therefore, the predicted ΔH should be 0. If, however, H_{20} is viewed at 80 cm, the adapting surface is perceived as concave. According to the curvature model, this would cause a subsequently viewed test surface (that appeared flat before adaptation) to appear convex now. As a consequence, ΔH should be positive. Similarly, if the observer adapts to H_{80} viewed at 80 cm, ΔH should be 0 whereas if the H_{80} is viewed at 20 cm, ΔH should be negative. If we interpolate these predictions with lines, we obtain the qualitative predictions of the curvature model shown in Fig. 3b.

In summary, the disparity model predicts that the curvature after-effect depends only on the second-order disparities and not on the adaptation distance. The curvature model, in contrast, predicts that the after-effect depends on the adaptation distance. Moreover, the disparity model predicts that the magnitude of the after-effect may depend on the test distance, whereas the curvature model predicts that the after-effect is independent of the test distance.

2. Methods

2.1. Observers

Four observers with normal or corrected to normal vision participated in the experiment. Two observers were naïve, and two were authors. Informed consent was obtained prior to participation.

2.2. Stimuli, apparatus and procedure

Stimuli were displayed on a haploscope consisting of two large monochrome CRT displays each seen in a mirror by one eye. Head position was fixed with a bite bar. A small target served as the fixation aid; it contained vertical nonius elements so observers could monitor their vergence accuracy. The stimuli consisted of sparse random-dot displays. Dot locations were specified to within 30 arcsec. This high level of spatial precision was achieved by use of antialiasing and spatial calibration (Backus, Banks, van Ee, & Crowell, 1999).

The dots were randomly distributed within an ellipse that subtended 30 deg horizontally and 1 deg vertically at the cyclopean eye. Because the vertical subtense was small, vertical disparities were not a reliable cue to distance (Rogers & Bradshaw, 1995; Backus et al., 1999). The dots were positioned in the two eyes such that the horizontal disparities specified a conic section (Fig. 2). Stimuli were presented at two simulated distances: 20 and 80 cm. The actual distance from each eye to the corresponding CRT was 40 cm. The only cue to simulated distance was the eyes' vergence. Vergence was manipulated by changing the horizontal position of the stimulus and fixation point on each CRT. This manipulation had no effect on the retinal images, so we could change vergence without changing the 2nd-order disparities.

In the first part of the experiment, observers were presented with a series of 1 s flashes of the test stimulus. They adjusted Huntil the stimulus appeared planar. The adaptation part of the experiment then began. The adaptation surface appeared at 20 or 80 cm with the desired curvature for 2 min. The texture on the surface changed every 10 s (without changing the disparity pattern) in order to minimize local light adaptation. The test stimulus was then flashed at a simulated distance of 20 or 80 cm for 1 s. This period was brief enough to minimize adaptation to the test stimulus, but was long enough to allow a complete vergence eye movement for the cases in which the test distance differed from the adaptation distance (Mitchell & Baker, 1973). The observer adjusted H in the test stimulus in the direction required to make it appear planar. Nulling the perceived curvature typically required several presentations and adjustments. After ev-

ery five presentations and adjustments, the adaptation stimulus reappeared for 10 s in order to maintain the magnitude of the after-effect. The difference between the pre- and post-adaptation H values that appeared planar (ΔH) was the measure of the curvature after-effect.

3. Results

Fig. 4 shows the average curvature after-effect (ΔH) for all conditions plotted as a function of the H value of the adaptation stimulus. ΔH is plotted as a function of the H value of the adapting stimulus. The unfilled symbols represent data obtained when the adaptation distance was 20 cm and the filled symbols data when the adaptation distance was 80 cm. The circles and squares represent data when the test distance was 20 and 80 cm, respectively. There is a clear effect of adaptation distance. Consider, for example, the data when observers adapted to H_{80}. Recall that H_{80} appears flat when viewed at 80 cm and concave when viewed at 20 cm, even though the patterns of retinal disparity are identical in the two cases. The after-effects created by H_{80} at the two adaptation distances are quite different: when the adaptation distance was 80 cm, no after-effect was observed ($\Delta H = 0$), and when the adaptation distance was 20 cm, a clear after-effect was observed ($\Delta H < 0$). These data are clearly consistent with the curvature model (see Fig. 3b) and not the disparity model. A similar observation occurred when the adapting stimulus was H_{20}; now, a clear after-effect was observed when this pattern of disparities was viewed at

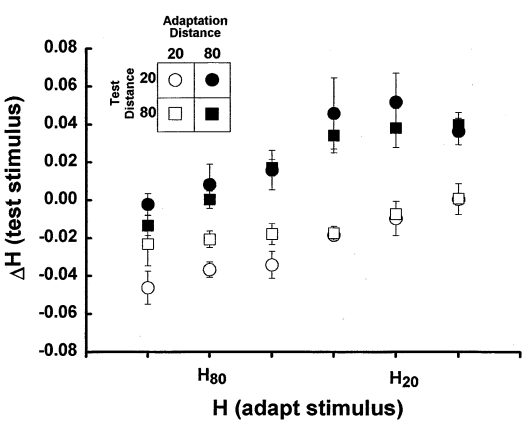

Fig. 4. Averaged results. The mean difference in the H value that looked planar before and after adaptation (ΔH) is plotted as a function of the H value of the adaptation stimulus. The unfilled circles represent the data for the condition in which the adaptation and test stimuli were presented at 20 cm. The unfilled squares represent the data for adaptation at 20 cm and test at 80 cm. The filled circles represent the data for adaptation at 80 cm and test at 20 cm. The filled squares represent the data for adaptation at 80 cm and test at 80 cm.

80 cm (where the stimulus appeared convex), but not 20 cm (where the stimulus appeared flat). Thus, the same pattern of disparity creates quite different after-effects, depending on the viewing distance during adaptation. This difference is clearly associated with the perceived curvature of the adapting stimulus, so the data support the curvature model.

Fig. 5 shows the same data plotted separately for each of the four observers. The same trends are evident in these data.

Fig. 6 plots the same data, but now the abscissa is the curvature of the adaptation stimulus rather than the disparity pattern. It can be seen that adapting stimuli of similar curvatures (but different disparity patterns) produced similar after-effects. Thus, the curvature of the adapting stimulus is a better predictor of the after-effect than is the disparity pattern.

A repeated-measure analysis of variance (ANOVA) was performed on the magnitude of the after-effect ΔH, with H ($H_{80}+\delta H$, H_{80}, $H_{80}+\delta H$, $H_{20}-\delta H$, H_{20}, $H_{20}+\delta H$), adaptation distance (20 and 80 cm), and test distance (20 and 80 cm) as within-subjects independent variables. We found significant main effects of H [$F(5,15) = 19.92$, $P < 0.01$] and adaptation distance [$F(1,3) = 31.33$, $P < 0.05$]. In addition, there were significant interactions between H and adaptation distance [$F(5,15) = 3.125$, $P < 0.05$], and between adaptation distance and test distance [$F(1,3) = 13.73$, $P < 0.05$].

4. Discussion

We found that the stereoscopic curvature after-effect is not predictable from the particular pattern of disparity (B) present in the adaptation stimulus. Rather, it depends on the 3D shape (curvature) of the stimulus. Our results indicate, therefore, that mechanisms representing 3D shape exist and are adaptable. It makes sense that shape-representing mechanisms exist because the estimation of 3D shape from the retinal images typically requires input from many relevant information sources. These sources include disparity and its gradients, motion parallax, texture gradients, eye-position signals, and more (Landy, Maloney, Johnston, & Young, 1995; Backus et al., 1999). The informativeness of the various sources depends heavily on viewing condition. For example, disparity is a very informative source for near surfaces, but is uninformative for far surfaces (Backus et al., 1999; Buckley & Frisby, 1993). Despite the variation in inputs from one viewing situation to another, the perceived shape of a surface typically remains much the same. Because we used short stimuli, only two variables contributed to perceived 3D curvature: the 2nd-order horizontal disparities and the vergence angle (Eq. (3)). With taller displays, vertical disparities would have also contributed (Rogers & Bradshaw, 1995; Backus et al., 1999).

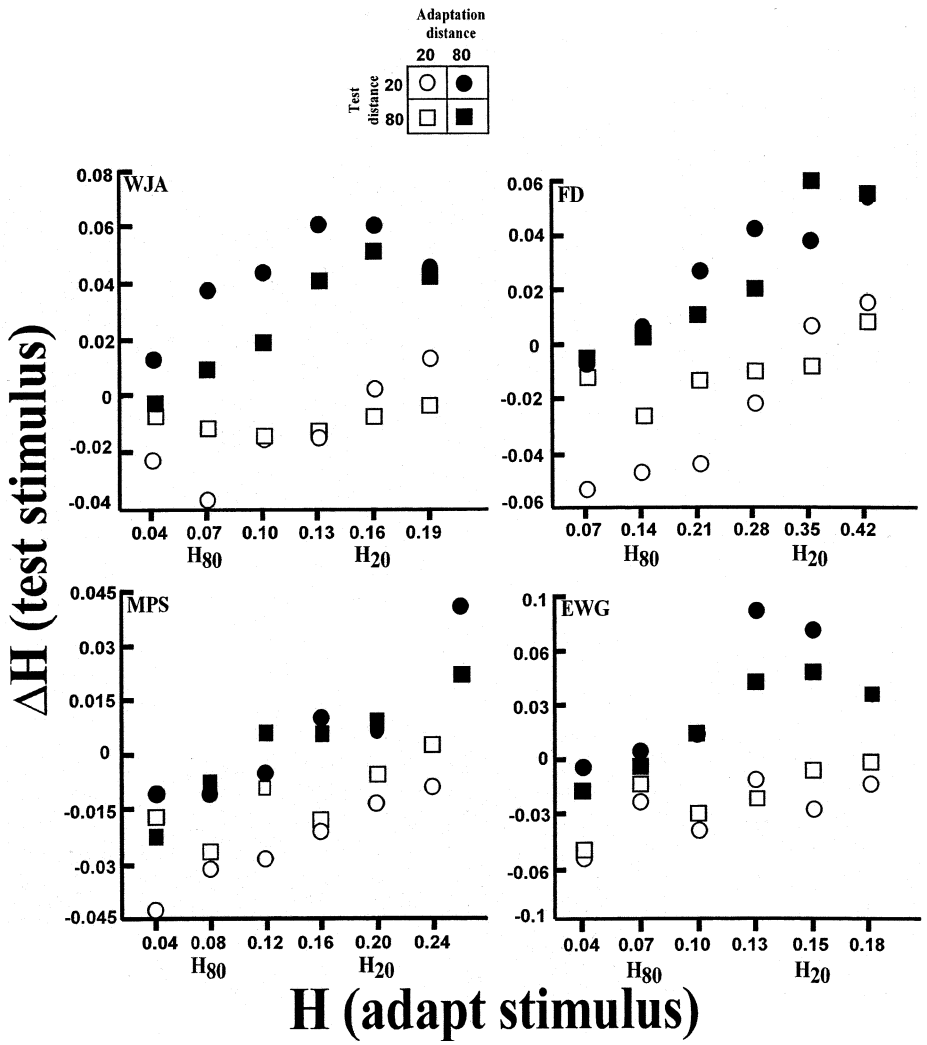

Fig. 5. Individual observers results. The difference in the H value that looked planar before and after adaptation (ΔH) is plotted as a function of the H value of the adaptation stimulus for each individual observer. The unfilled circles represent the data for the condition in which the adaptation and test stimuli were presented at 20 cm. The unfilled squares represent the data for adaptation at 20 cm and test at 80 cm. The filled circles represent the data for adaptation at 80 cm and test at 20 cm. The filled squares represent the data for adaptation at 80 cm and test at 80 cm.

It is well known that the perceived size of a stimulus may change with vergence distance (Howard & Rogers, 1995). This effect is called vergence micropsia. Could a change in perceived size have affected perceived curvature via vergence micropsia and thereby affected the interpretation of the data? It could not because the task was to adjust the disparity pattern until the test stimulus appeared planar. A change in the perceived size of a planar surface would not affect its perceived curvature, so our data are immune to such a potential confound.

It is easier to understand the present findings if we suppose that there are mechanisms that represent surface shape independent from the information source(s) specifying the shape. Recent work by Poom and Boerjesson (1999) supports this idea. They found that adaptation to a plane whose slant was specified by disparity produced an after-effect on a plane whose

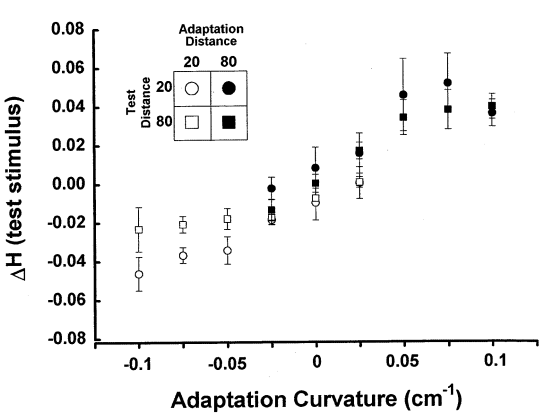

Fig. 6. Averaged results in terms of surface curvature. The data from Fig. 4 replotted in terms of curvature. ΔH averaged across observers is plotted as a function of the curvature of the adaptation stimulus.

slant was specified by a monocular depth cue. Moreover, Bradshaw and Rogers (1996) found that there is a substantial elevation for detecting the 3D structure of corrugated surfaces defined by either binocular disparity or motion parallax following adaptation to surfaces defined by either the same or different cue (but see also Graham & Rogers, 1982). Recent physiological findings also show that shape-representing mechanisms exist in the extrastriate cortex. For example, Sakata et al. (1999) have shown that visually responsive neurons in area AlP encode surface tilt (the direction of slant) whether the tilt is specified by disparity alone, monocular cues alone, or both. Moreover, Janssen, Vogels, and Orban (1999) have shown that some neurons in inferior temporal cortex are tuned to shape rather than disparity gradients. According to them, approximately one-third of IT cells respond selectively to particular 3D shapes, and the response selectivity is unchanged when the distance to the stimulus is varied in a way that alters the input disparities.

In conclusion, we have developed a technique that allows one to examine whether the mechanisms involved in depth after-effects are tuned to particular disparity patterns or to 3D shape curvature. The results indicated that the primary determinant is shape and not disparity pattern. As such, the results seem to reflect the workings of mechanisms that represent the 3D shape of a surface independent from the particular set of signals specifying the shape.

Acknowledgements

The authors thank Mike Landy and Pascal Mamassian for comments on an earlier draft. This research was supported by research grants from NSF (DBS-9309820) and AFOSR (93NL366) and a training grant from NIH (T32 EY0704).

References

Backus, B. T., Banks, M. S., van Ee, R., & Crowell, J. A. (1999). Horizontal and vertical disparity, eye position, and stereoscopic slant perception. *Vision Research*, *39*, 1143–1170.

Bradshaw, M. F., & Rogers, B. J. (1996). The interaction of binocular disparity and motion parallax in the computation of depth. *Vision Research*, *36*, 3457–3468.

Buckley, D., & Frisby, J. P. (1993). Interaction of stereo, texture and outline cues in the shape perception of three-dimensional ridges. *Vision Research*, *33*, 919–933.

Howard, I. P., & Rogers, B. J. (1995). *Binocular vision and stereopsis*. Oxford: Oxford University Press.

Graham, M., & Rogers, B. (1982). Simultaneous and successive contrast effects in the perception of depth from motion-parallax and stereoscopic information. *Perception*, *11*, 247–262.

Koehler, W., & Emery, D. A. (1947). Figural after-effects in the third dimension of visual space. *American Journal of Psychology*, *60*, 159–201.

Janssen, P., Vogels, R., & Orban, G. A. (1999). Macaque inferior temporal neurons are selective for disparity-defined three-dimensional shapes. *Proceedings of the National Academy of Sciences*, *96*, 8217–8222.

Landy, M. S., Maloney, L. T., Johnston, E. B., & Young, M. (1995). Measurement and modeling of depth cue combination: in defense of weak fusion. *Vision Research*, *35*, 389–412.

Long, N. R., & Over, R. (1973). Stereoscopic depth aftereffects with random-dot patterns. *Vision Research*, *13*, 1283–1287.

McCollough, C. (1965). Colour adaptation of edge-detectors in the human visual system. *Science*, *149*, 1115.

Mitchell, D. E., & Baker, A. G. (1973). Stereoscopic aftereffects: evidence for disparity-specific neurones in the human visual system. *Vision Research*, *13*, 2273–2288.

Ogle, K. N. (1950). *Researches in binocular vision*. Philadelphia, PA: W.B. Saunders.

Poom, L., & Bocijesson, E. (1999). Perceptual depth synthesis in the visual system as revealed by selective adaptation. *Journal of Experimental Psychology: Human Perception and Performance*, *25*, 504–517.

Ryan, C., & Gillam, B. (1993). A proximity-contingent stereoscopic depth aftereffect: evidence for adaptation to disparity gradients. *Perception*, *22*, 403–418.

Rogers, B. J., & Bradshaw, M. F. (1995). Disparity scaling and the perception of frontparallel surfaces. *Perception*, *24*, 155–179.

Sakata, H., Taira, M., Kusunoki, M., Murata, A., Tsutsui, K., Tanaka, Y., Shein, W. N., & Miyashita, Y. (1999)). Neural representation of three-dimensional features of manipulation objects with stereopsis. *Experimental Brain Research*, *128*, 160–169.

te Pas, S. F., Rogers, B. J., & Ledgeway, T. (1997)). A curvature contrast effect for stereoscopically defined surfaces. *Perception*, *26*, 30.

von Helmholtz, H. (1909). *Physiological optics*. New York: Dover 1962 English translation by J.P.C. Southhall from the 3rd German edition of Handbuch der Physiologischen Optik. Hamburg: Vos.